Pis'ma v ZhETF, vol. 95, iss. 1, pp. 13 – 16 © 2012 January 10

Effects of intermodal dispersion on short pulse propagation in multi-core fibers

M. Liu[1)], *D. Li*, *Zh. Liao*

College of Communication Engineering, Chongqing University, Chongqing, China

Submitted 21 October 2011

Resubmitted 18 November 2011

The effects of intermodal dispersion on ultrashort optical pulse propagation through multi-core fibers are analyzed theoretically, which has been ignored in previous studies. A three-core fiber with collinear and triangular configuration and a four-core fiber are considered. We demonstrate with numerical examples that the intermodal dispersion can cause pulse breakup effect in multi-core fibers.

1. Introduction. It was demonstrated by Finlayson and Stegeman that a three-core nonlinear directional coupler can offer some distinct advantages over the two-core coupler [1]. In particular, by comparison with the two-waveguide coupler, three-waveguide couplers have more output states, markedly sharper switching characteristics, and display greater sensitivity to the input state [2]. Recently, the nonlinear three-core couplers based on a photonic crystal fiber (PCF) have been shown that the three-core PCF reveals many novel characteristics and is capable of realizing polarization splitter, mode splitter, and novel WDM demultiplexer [3–7].

It has been shown that the intermodal dispersion can affect significantly the propagation of ultra-short pulses in the two-core fiber [8–16]. It's expected that the intermodal dispersion, caused by the difference between the group delays of two modes, should exist in multi-core (three-core and four-core) fiber. However, so far, the studies on multi-core fibers have neglected the effects of the intermodal dispersion. In this Letter, different pulse switching dynamics in multi-core fibers are investigated and the effects of intermodal dispersion on short pulse propagation in multi-core fibers are highlighted.

2. Analysis and Discussion. We consider a three-core fiber with both the collinear and triangular configuration and a four-core fiber as shown in Fig. 1. The normalized coupled-mode equations that describe the propagation of ultrashort pulses in a collinear three-core fiber are expressed as Eqs. (1)–(3):

$$i\frac{\partial A_1}{\partial Z}+\frac{1}{2}\frac{\partial^2 A_1}{\partial T^2}+|A_1|^2A_1+RA_2+iR'\frac{\partial A_2}{\partial T}=0, \quad (1)$$

$$i\frac{\partial A_2}{\partial Z}+\frac{1}{2}\frac{\partial^2 A_2}{\partial T^2}+|A_2|^2A_2+R(A_1+A_2)+ +iR'\left(\frac{\partial A_1}{\partial T}+\frac{\partial A_3}{\partial T}\right)=0, \quad (2)$$

$$i\frac{\partial A_3}{\partial Z}+\frac{1}{2}\frac{\partial^2 A_3}{\partial T^2}+|A_3|^2A_3+RA_2+iR'\frac{\partial A_2}{\partial T}=0, \quad (3)$$

where A_1, A_2 and A_3 are the normalized amplitudes of the modes in the individual cores, respectively [13]; $Z=z/L_D$ and $T=(t-z/v_g)/T_0$ are the normalized distance and retarded-time coordinates, respectively (with z and t the actual distance and time, respectively), where $L_D=-T_0^2/\beta_2$ is the dispersion length with $\beta_2(<0)$ the group-velocity dispersion, v_g is the group velocity, and T_0 is a characteristic width of the input pulse; $R=-T_0^2C/\beta_2$ and $R'=-T_0C'/\beta_2$ [13] are the normalized coupling coefficient and coupling-coefficient dispersion or intermodal dispersion, respectively, where C is the coupling coefficient and (with ω the angular optical frequency) is a measure of the wavelength dependence of the coupling coefficient. The terms with R' in Eqs. (1)–(3) account for the intermodal dispersion.

In our study, we assume that a pulse is launched into only one core, i.e., $A_1(0,T)=A\mathrm{sech}(T)$, $A_2(0,T)=A_3(0,T)=0$, where A is the normalized amplitude of the input pulse and the peak power of the pulse is $P_0=|A|^2$. We solve the coupled-mode equations numerically by a Fourier series analysis method [15].

Figure 2 shows the evolution of the normalized pulse envelopes in a collinear three-core fiber. The results are calculated for $R=10$ with intermodal dispersion $R'=0$ and $R'=-6$, respectively, where $U=|A_1|^2/A^2$,

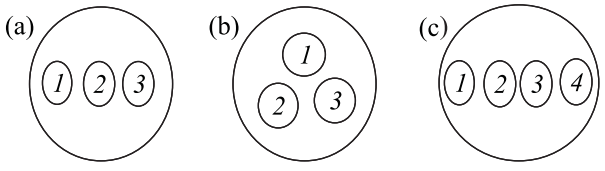

Fig. 1. Schematics of the three-core and four-core fiber configuration: collinear three-core fiber (a), triangular three-core fiber (b) and four-core fiber (c)

[1)] e-mail: liumin_mm@yahoo.com

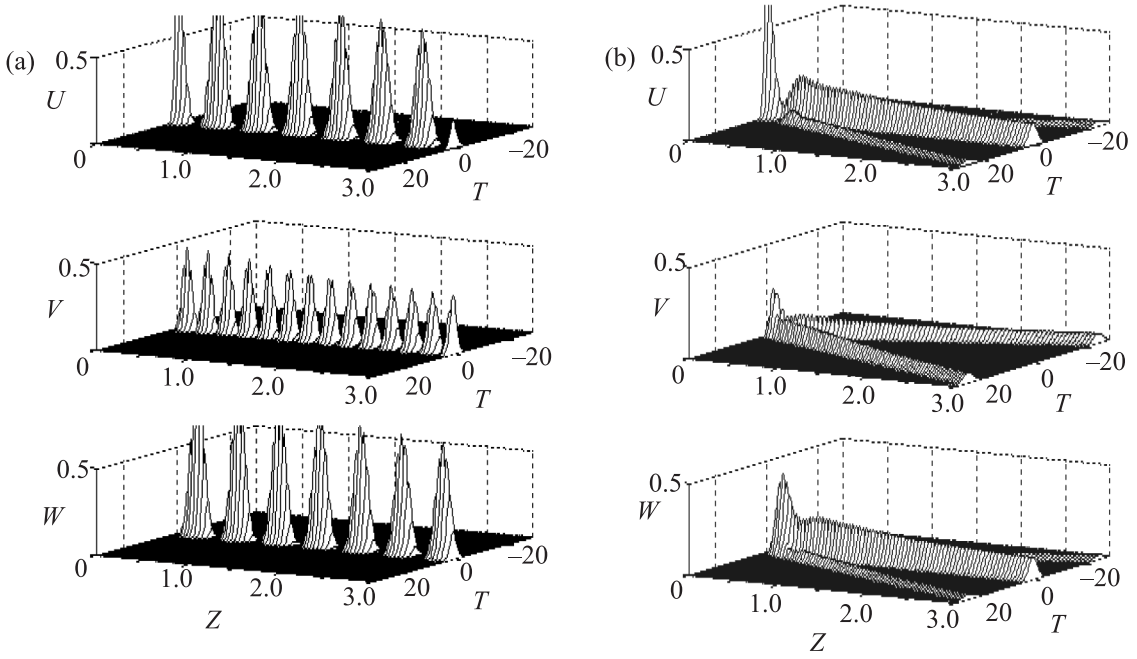

Fig. 2. Pulse propagation in a collinear three-core fiber for $R = 10$ with $R' = 0$ (a) and $R' = -6$ (b)

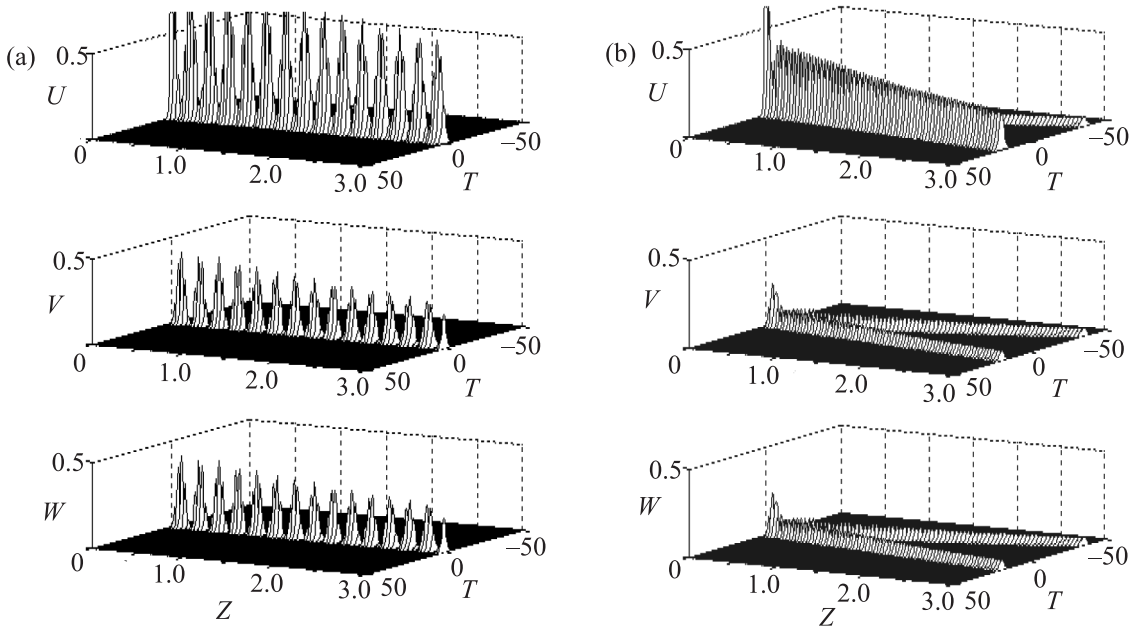

Fig. 3. Pulse propagation in a triangular three-core fiber for $R = 10$ with $R' = 0$ (a) and $R' = -6$ (b)

$V = |A_2|^2/A^2$, $W = |A_3|^2/A^2$ are the normalized power envelopes of the pulses. The values $R' = -6$ correspond roughly to the situation of propagating $a \sim 100$-fs pulse at the wavelength $1.55\,\mu$m in a two-core fiber with a center- to-center core separation approximately 5 times the core radius [10]. As shown in Fig. 2a, in the absence of intermodal dispersion, the pulse can switch back and forth in three cores without pulse distortion. However, when intermodal dispersion is included, the switching dynamics changes greatly. As can be seen from Fig. 2b, we can observe that two small pulses emerge from Core 2, and the output pulse from Core 1 and Core 3 are identical, where three pulses emerge from the output and their group velocity are different. This is because

there are three supermodes in the fiber, which has different field distributions in three cores. Due to the intermodal dispersion, these supermodes propagate at different group velocities. The three sets of pulses at the output of the fiber shown in Fig. 2 correspond to the three separated supermodes, respectively.

The normalized coupled-mode equations for a triangular three-core fiber are given by:

$$i\frac{\partial A_1}{\partial Z}+\frac{1}{2}\frac{\partial^2 A_1}{\partial T^2}+|A_1|^2A_1+R(A_2+A_3)+ +iR'\left(\frac{\partial A_2}{\partial T}+\frac{\partial A_3}{\partial T}\right)=0, \quad (4)$$

$$i\frac{\partial A_2}{\partial Z}+\frac{1}{2}\frac{\partial^2 A_2}{\partial T^2}+|A_2|^2A_2+R(A_1+A_3)+ +iR'\left(\frac{\partial A_1}{\partial T}+\frac{\partial A_3}{\partial T}\right)=0, \quad (5)$$

$$i\frac{\partial A_3}{\partial Z}+\frac{1}{2}\frac{\partial^2 A_3}{\partial T^2}+|A_3|^2A_3+R(A_1+A_2)+ +iR'\left(\frac{\partial A_1}{\partial T}+\frac{\partial A_2}{\partial T}\right)=0, \quad (6)$$

The terms follow those defined in Eqs. (1)–(3). The pulse propagation in a triangular three-core fiber for $R=10$ with $R'=0$ and $R'=-6$ are shown in Figs. 3a and b respectively. It can be seen that clear pulse switching dynamics occurs without the consideration of intermodal dispersion. In the presence of intermodal dispersion, we can observe the pulse break up effect simultaneously in three cores. Due to the symmetry of a triangular three-core fiber, the output pulse from Core 2 and Core 3 are identical.

As for collinear four-core fibers, the optimized configuration with unequal core spacing is studied. When the separation between the middle two cores is made smaller so that the coupling coefficient between the middle two cores is larger than that of the two side cores by a factor of $2/\sqrt{3}$, 100% power transfer from the first core to the fourth core becomes possible. The normalized coupled-mode equations are:

$$i\frac{\partial A_1}{\partial Z}+\frac{1}{2}\frac{\partial^2 A_1}{\partial T^2}+|A_1|^2A_1+\sqrt{3}RA_2+i\sqrt{3}R'\frac{\partial A_2}{\partial T}=0, \quad (7)$$

$$i\frac{\partial A_2}{\partial Z}+\frac{1}{2}\frac{\partial^2 A_2}{\partial T^2}+|A_2|^2A_2+R(\sqrt{3}A_1+2A_3)+ +iR'\left(\sqrt{3}\frac{\partial A_1}{\partial T}+2\frac{\partial A_3}{\partial T}\right)=0, \quad (8)$$

$$i\frac{\partial A_3}{\partial Z}+\frac{1}{2}\frac{\partial^2 A_3}{\partial T^3}+|A_3|^2A_3+R(2A_2+\sqrt{3}A_4)+ +iR'\left(2\frac{\partial A_2}{\partial T}+\sqrt{3}\frac{\partial A_4}{\partial T}\right)=0, \quad (9)$$

$$i\frac{\partial A_4}{\partial Z}+\frac{1}{2}\frac{\partial^2 A_4}{\partial T^2}+|A_4|^2A_4+\sqrt{3}RA_3+i\sqrt{3}R'\frac{\partial A_3}{\partial T}=0. \quad (10)$$

The input condition is: $A_1(0,T)=A\mathrm{sech}(T)$, $A_2(0,T)=A_3(0,T)=A_4(0,T)=0$. The switching dynamics of a four-core fiber with $R=10$ for $R'=0$ and $R'=-6$ are shown in Figs. 4a and b respectively,

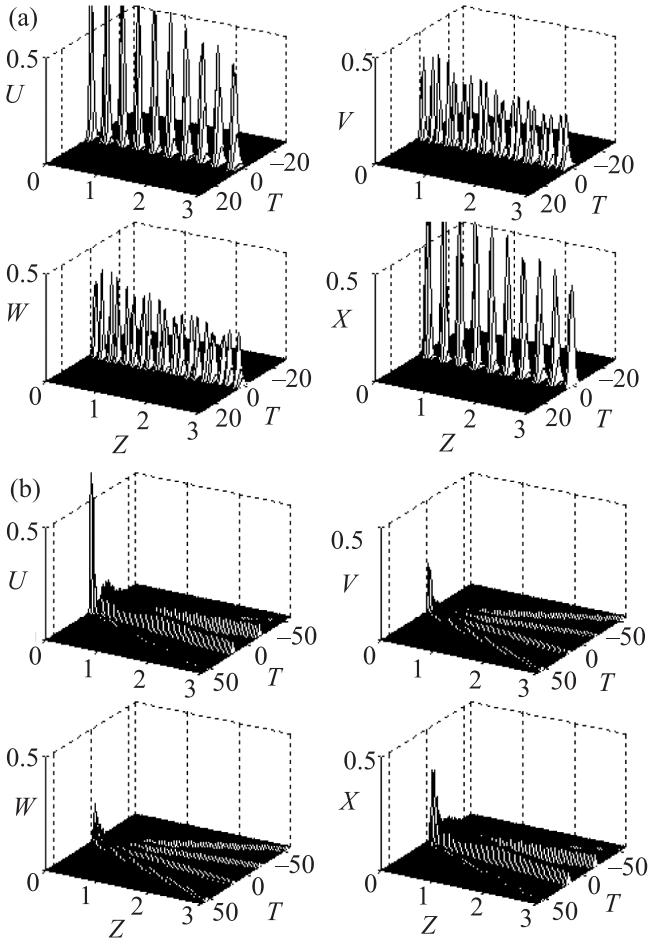

Fig. 4. Pulse propagation in a four-core fiber for $R=10$ with $R'=0$ (a) and $R'=-6$ (b)

where $U=|A_1|^2/A^2$, $V=|A_2|^2/A^2$, $W=|A_3|^2/A^2$, and $X=|A_4|^2/A^2$. Comparing Fig. 4a with Fig. 4b, we can see that in the presence of intermodal dispersion, the input pulse splits into separate pulses in four cores completely. As shown in Fig. 4b, two pulses with equal powers emerge from Core 1 and Core 4, while four small pulses with equal powers emerge from Core 2 and Core 3. There exists group delay difference between subpulses. This can be understood in that there are four supermodes in the fiber, which has different

field distributions in four cores. Owing to intermodal dispersion, these supermodes propagate along the fiber at different group velocities. The four sets of pulses at the output of the fiber shown in Fig. 4 correspond to the four separated supermodes, respectively.

3. Conclusion. By solving a set of generalized, linearly coupled nonlinear Schrodinger equations including intermodal dispersion, the pulse switching dynamics of nonlinear three-core (collinear and triangular) and four-core fibers are analyzed. We find that when the input pulse is shorter than a few hundred femtoseconds, the intermodal dispersion in the fiber can lead to splitting of the input pulse into sets of smaller pulses emerging from all the cores of the fiber over a short distance. Our results will be very useful for the design of more realistic multi-core fibers with seven or more cores.

The research was supported by the Fundamental Research Funds for the Central Universities, Project # CDJZR10 16 00 06.

1. N. Finlayson and G.I. Stegeman, Applied Phys. Lett. **56**, 2276 (1990).
2. J.M. Soto-Crespo and E.M. Wright, J. Appl. Phys. **70**, 7240 (1991).
3. M.I. Molina, W.D. Deering, and G.P. Tsironis, Phys. D. **66**, 135 (1993).
4. K. Saitoh, Y. Sato, and M. Koshiba, Opt. Express **12**, 3940 (2004).
5. Zh. Wang, Y. Wang, Y. Li, and Ch. Wu, Opt. Express **14**, 10324 (2006).
6. M.-Y. Chen, J. Zhou, and E.Y.B. Pun, J. Lightwave Techno. **27**, 2343 (2009).
7. P. Li, J.L. Zhao, and X.J. Zhang, Opt. Express **18**, 26828 (2010).
8. K.S. Chiang, Opt. Lett. **20**, 997 (1995).
9. K.S. Chiang, IEEE J. Quantum Electron. **33**, 950 (1997).
10. P. Shum, K.S. Chiang, and W.A. Gambling, IEEE J. Quantum Electron. **35**, 79 (1999).
11. P.M. Ramos and C.R. Paiva, J. Opt. Soc. Am. B **17**, 1125 (2000).
12. P. Peterka, P. Honzatko, J. Kanka et al., Proc. SPIE **5036**, 376 (2003).
13. M. Liu, K.S. Chiang, and P. Shum, IEEE J. Quantum Electron. **40**, 1597 (2004).
14. M. Liu, K.S. Chiang, and P. Shum, Opt. Commun. **219**, 171 (2003).
15. M. Liu and K.S. Chiang, Appl. Phys. B, **98**, 815 (2010).
16. M. Liu and K.S. Chiang, Opt. Express **18**, 21261 (2010).